Nuclear Instruments and Methods in Physics Research A 707 (2013) 26–34

Contents lists available at SciVerse ScienceDirect

Nuclear Instruments and Methods in Physics Research A

journal homepage: www.elsevier.com/locate/nima

Performance evaluation and optimization of the MiniPET-II scanner

Imre Lajtos [a,*], Miklos Emri [a], Sandor A. Kis [a], Gabor Opposits [a], Norbert Potari [a], Beata Kiraly [b], Ferenc Nagy [b], Lajos Tron [a], Laszlo Balkay [a]

[a] Department of Nuclear Medicine, Medical and Health Science Center, University of Debrecen, 4032 Debrecen, Nagyerdei krt. 98, Hungary
[b] Institute of Nuclear Research of the Hungarian Academy of Sciences, Debrecen, 4026 Debrecen, Bem tér 18/c, Hungary

A R T I C L E   I N F O

Article history:
Received 26 April 2012
Received in revised form
3 December 2012
Accepted 10 December 2012
Available online 21 December 2012

Keywords:
Small-animal PET scanner
Image quality
Coincidence time window
NEMA
Preclinical imaging

A B S T R A C T

This paper presents results of the performance of a small animal PET system (MiniPET-II) installed at our Institute. MiniPET-II is a full ring camera that includes 12 detector modules in a single ring comprised of $1.27 \times 1.27 \times 12$ mm^3 LYSO scintillator crystals. The axial field of view and the inner ring diameter are 48 mm and 211 mm, respectively. The goal of this study was to determine the NEMA-NU4 performance parameters of the scanner. In addition, we also investigated how the calculated parameters depend on the coincidence time window (τ=2, 3 and 4 ns) and the low threshold settings of the energy window (E_{lt}=250, 350 and 450 keV). Independent measurements supported optimization of the effective system radius and the coincidence time window of the system. We found that the optimal coincidence time window and low threshold energy window are 3 ns and 350 keV, respectively. The spatial resolution was close to 1.2 mm in the center of the FOV with an increase of 17% at the radial edge. The maximum value of the absolute sensitivity was 1.37% for a point source. Count rate tests resulted in peak values for the noise equivalent count rate (NEC) curve and scatter fraction of 14.2 kcps (at 36 MBq) and 27.7%, respectively, using the rat phantom. Numerical values of the same parameters obtained for the mouse phantom were 55.1 kcps (at 38.8 MBq) and 12.3%, respectively. The recovery coefficients of the image quality phantom ranged from 0.1 to 0.87. Altering the τ and E_{lt} resulted in substantial changes in the NEC peak and the sensitivity while the effect on the image quality was negligible. The spatial resolution proved to be, as expected, independent of the τ and E_{lt}. The calculated optimal effective system radius (resulting in the best image quality) was 109 mm. Although the NEC peak parameters do not compare favorably with those of other small animal scanners, it can be concluded that under normal counting situations the MiniPET-II imaging capability assures remarkably good image quality, sensitivity and spatial resolution.

1. Introduction

During the last two decades, a number of dedicated animal PET scanners were constructed and used for preclinical investigations either at university or pharmaceutical/biological industry sites. The Concorde micro-PET, the first commercial (in 2000) small animal PET camera, was originally designed and developed at the University of California, Los Angeles [1,2]. At that time, characterization of the performance of small animal scanners and comparisons of the different systems was possible only by applying custom based protocols using the National Electrical Manufacturers Association (NEMA) standards for human PET cameras. There was a strong demand for standardization of the performance tests of small animal PET scanners [3], and as a result a new NEMA NU-4 standard was introduced to this field in 2008 [4].

After the release of this standard, a number of publications appeared reporting on results obtained using NEMA NU-4 performance tests protocols. Some of these studies accomplished the complete tests on dedicated small animal PET systems [5–9,21,23,27] while others utilized the instructions of NEMA NU-4 standard also to optimize performance test parameters under different imaging conditions including application of different image reconstruction methods. There were publications, among others, analyzing the effect of the attenuation correction and reconstruction [10], the normalization [11], the type of positron emitter [12] and the object size [13] on the performance test parameters. Further studies were carried out using the NEMA NU-4 IQ (NU4IQ) phantom to optimize the parameter settings of the reconstruction [14] and the acquisition [15] in order to obtain the best values of homogeneity, recovery coefficient (RC) and spill-over ratio (SOR).

At our Institute, a full ring small animal PET camera (MiniPET-II) has been built as a part of a research and development project and the performance parameters were evaluated with the NEMA

* Corresponding author. Tel./fax: +36 52 255500.
E-mail addresses: lajti@pet.dote.hu, lajti00@gmail.com (I. Lajtos).

0168-9002/$ - see front matter © 2012 Elsevier B.V. All rights reserved.
http://dx.doi.org/10.1016/j.nima.2012.12.079

NU-4 standards [16]. The measured and calculated parameters characterize the actual PET scanner well, however, they may depend on the basic settings of the PET system. Certain parameter settings or procedures cannot be altered at all (e.g. number of crystals, axial field of view), while others (energy window, coincidence time window, algorithm and parameters of the reconstruction) can be changed both before the data acquisition and/or during the data processing. One of the basic reconstruction parameters is the effective radius (R_e) of the scanner, which stands for the presumed distance between the axis of the scanner and the photoelectric interaction point (interaction centroid) in the crystal. This value is obviously larger than the scanner inner radius. In addition, previous studies demonstrated that the interaction centroid does not correspond to the geometrical centers of the crystals [17]. It was also shown that an inaccurate effective radius could generate distortions in the reconstructed image [17].

In the present study we investigated the dependence of the calculated performance parameters (like spatial resolution, sensitivity, etc.) on the coincidence time window (τ), and on the low threshold settings of the energy window (E_{lt}). In addition, using a Micro Deluxe type phantom we also demonstrated that the reconstructed image contrast can be improved by optimization of the presumed effective system radius.

2. Methods

2.1. System description

The measurements were carried out on the MiniPET-II small animal scanner. This system includes 12 detector modules (arranged in a single ring) with LYSO (PreLude™ 420, $Lu_{1.8}Y_{.2}SiO_5$:Ce, $\mu = 0.83\ cm^{-1}$) scintillator crystal blocks and position sensitive Hamamatsu H9500 PMTs. Fig. 1 shows the design and the layout of the MiniPET-II scanner. The most important physical and geometrical data are displayed in Table 1. Each PMT has 256 anodes and these readout channels are reduced to 4 by a resistive charge division network. The four detector signals are digitized by custom made data acquisition cards with four triggerless ADC inputs. The digitized signals are fed to a Xilinx Virtex4 field-programmable gate array (FPGA) board where time stamp generation, energy calculation, signal recognition and status check processes take place. A central clock generator provides the 50 MHz clock signal for the modules. The FPGA also performs rough coincidence discrimination to assure the prefiltering of the input events. The data from the detector modules are transmitted to the data acquisition PC via the 100BASE-TX Ethernet network. A custom made software library, the MultiModal Medical Imaging (M3I) was developed [18] in order to handle each emerging task of data collection and processing (primary data processing, scanner calibration, image reconstruction, image processing and evaluation of performance parameters as well). This software tool enables arranging data in 3D LOR or single events list mode data files. 3D LOR files can be histogrammed into 2D sinograms or 2D LOR sets. The M3I library supports reconstruction algorithms 2D FBP, iterative 2D ML-EM and OSEM, and it comprises the delayed random correction and component based normalization [19,20].

Measurements and data evaluations were performed according to the NEMA standard protocol using three different values for both τ (2, 3 and 4 ns) and E_{lt} (250 keV, 350 keV, and 450 keV).

2.2. Spatial resolution

The spatial resolution of an imaging system characterizes its ability to distinguish between two points on the reconstructed

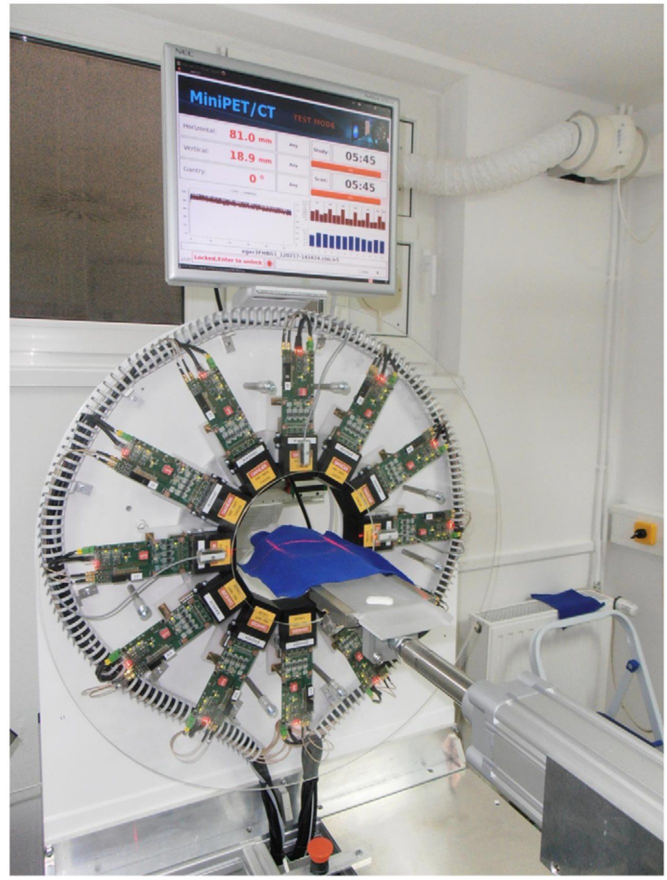

Fig. 1. The MiniPET-II system.

Table 1
Basic physical properties of the MiniPET-II system.

Scintillator material	LYSO
Crystal size (mm^3)	$1.27 \times 1.27 \times 12$
Crystal pitch (mm)	1.347
Crystal array size	35×35
PMT type	Hamamatsu H9500
Energy resolution (%)	17
Number of PMT	12
Number of detector block	12
Number of crystal ring	35
Diameter of ring (mm)	211
Solid angle/4π	0.22
Trans-axial FOV (mm)	100
Axial FOV (mm)	48

image. Data acquisitions used for the determination of this parameter were performed using a small volume source ($0.3 \times 0.3 \times 0.3\ mm^3$). The NEMA-NU4 standard requires a ^{22}Na point source in acryl cube of $10 \times 10 \times 10\ mm^3$ size, nevertheless we used a ^{18}F source in glass capillary. The length of the source, the inner and outer radius of the capillary were 0.3, 0.15 and 0.75 mm, respectively; the activity of the source was 90 kBq. The measurements were carried out in 12 predefined locations within the field of view at the axial center and along the axis at a distance of 1/4 of the axial length from the center of the FOV (referred to as 1/4 axial center) and the scan time was set to 2 min in each position. The effect of the energy and coincidence discrimination on the spatial resolution was also examined. The measured data were rebinned using the single-slice rebinning (SSRB) method (number of projections was 210). The rebinned